Review of Local Buckling Width-to-Thickness Limits

BEN W. SCHAFER, LOUIS F. GESCHWINDNER, TOM SABOL, and CHIA-MING UANG

ABSTRACT

This paper provides a review of local buckling width-to-thickness limits (also known as *w/t* or λ) employed in the ANSI/AISC 360-16 *Specification for Structural Steel Buildings* (2016b), hereafter referred to as AISC 360, and ANSI/AISC 341-16 *Seismic Provisions for Structural Steel Buildings* (2016a), hereafter referred to as AISC 341. The review was conducted by a task group formed to address potential changes in the next and/or future editions of the AISC *Specifications*. A comprehensive review of existing local buckling limits was completed, including detailing the underlying assumptions and the objectives of the existing limits. In addition, particular attention was given to the potential impact of adopting newer steel materials on the local buckling limits and to considerations of web-flange interaction in local buckling. Further, new methods that have been developed to address local buckling in structural steel design were also examined. It was found that in AISC 360, some λ_r limits for flexure may not be well aligned with intended objectives, and while all λ_p limits for flexure ensure the plastic moment may be achieved, rotation objectives are not consistently implemented. Review of λ_{md} and λ_{hd} in AISC 341 reveals complications with implementing expected yield stress in the slenderness parameters and highlights the large number of varied objectives for these limits in seismic design, as well as a need for improvements—particularly for deep wide-flange columns. In general, it is found that only minor changes are potentially needed to current width-to-thickness, *w/t*, limits. Thus, in most cases, it is expected that AISC design can continue unchanged, with the exception of the improved criteria for deep columns. To minimize change while still expanding opportunity, newer local buckling cross-section classification methods could be permitted as alternatives rather than used as replacements to current *w/t* limits so that advantages of the newer approaches can be utilized when beneficial.

INTRODUCTION

During the development of the 2022 editions of AISC 360 (2016b) and AISC 341 (2016a), the AISC Committee on Specifications determined that a review of current local buckling width-to-thickness limits (also known as *w/t* or λ) would be useful and appointed a task group, of which the first author was chair, to study the issue. Concerns about web-flange interaction in the cyclic response of deep columns, a desire to be forward-thinking regarding the adoption of higher strength steels, and an interest in alternative methods that had been developed to address local buckling were some of the motivating reasons for the formation of the task group. The task group was charged with reviewing all existing *w/t* limits, explicitly stating the objective of these limits and if current criteria achieve desired objectives, examining the impact of material properties and web-flange interaction on the *w/t* limits, exploring alternatives to current methods for local buckling control, and finally to provide recommendations for the next and future editions of the AISC 360 and 341 *Specifications*. The objective of this paper is to provide a summary of the task group's report from Schafer et al. (2020).

Ben W. Schafer, Professor, Johns Hopkins University, Baltimore, Md. Email: schafer@jhu.edu (corresponding)

Louis F. Geschwindner, Professor Emeritus, Pennsylvania State University, State College, Pa. Email: lfg@psu.edu

Tom Sabol, Adjunct Professor, University of California–Los Angeles, Los Angeles, Calif. Email: tsabol@ucla.edu

Chia-Ming Uang, Professor, University of California–San Diego, San Diego, Calif. Email: cmu@ucsd.edu

Paper No. 2021-04

BACKGROUND

Classically, steel cross sections are conceptualized as being composed of a series of connected long plates. The plates (also known as elements) of the cross section with continuous connection along both longitudinal edges, such as the web of an I-section, are known as stiffened elements; while plates with connection along only one longitudinal edge, such as half the flange of an I-section, are known as unstiffened elements. The elastic buckling of long plates, using Kirchoff thin plate theory (Allen and Bulson, 1980), leads to the following classical expression:

$$F_{cr} = k\frac{\pi^2 E}{12(1-\nu^2)}\left(\frac{t}{w}\right)^2 \tag{1}$$

where F_{cr} is the elastic plate buckling stress; E is the material modulus of elasticity; ν is the material Poisson's ratio; t and w define the plate thickness and width, respectively; and the plate buckling coefficient, k, is a function of the loading and boundary conditions. Solutions for k exist for a wide variety of conditions and can consider multiple attached elements to form a full cross section (Allen and Bulson, 1980; Seif and Schafer, 2010; Gardner et al., 2019). However, only the simplest values are commonly used in design—for example, k of 4 for a stiffened element in uniform compression or k of 0.425 for an unstiffened element in uniform compression. See Allen and Bulson (1980), Salmon et al. (2009), and Ziemian (2010) for further discussion and a more thorough background.

Structural steel design specifications worldwide use w/t limits to provide engineers with guidance on the impact of local buckling on their designs. The strength and/or curvature capacity of beams is the archetypical case for this application and is illustrated in Figure 1, which includes the nomenclature of AISC 360: slender, noncompact, and compact, as well as that of Eurocode/EN 1993 (CEN, 2004): Class 4, Class 3, Class 2, and Class 1, where M_y is the moment at first yield, M_p the plastic moment, κ the curvature, and κ_p the plastic curvature of the beam when M_p is first reached.

If local plate buckling behaved in a manner similar to global flexural buckling (post-buckling neutral), then w/t limits would be easy to establish because elastic buckling itself would provide a useful limit. However, unlike flexural buckling of a member, local buckling of a plate is not post-buckling neutral—local plate buckling is post-buckling stable. Thus, design rules do not generally use F_{cr} for the plate as directly as one would use for flexural buckling. Further, the elastic plate buckling provides no consideration for material nonlinearity in the form of Equation 1. Therefore, development of w/t limits has classically relied on comparisons to experimental testing. If one can establish a buckling stress—say, at a stress of aF_y—that meets a desired objective (e.g., M_p, a target rotation, etc.), then the resulting w/t limit can be simplified as follows:

$$F_{cr} = k\frac{\pi^2 E}{12(1-\nu^2)}\left(\frac{t}{w}\right)^2 = aF_y \tag{2}$$

$$\left(\frac{w}{t}\right)_{limit} = \sqrt{\frac{k\pi^2}{a12(1-\nu^2)}}\sqrt{\frac{E}{F_y}} = C\sqrt{\frac{E}{F_y}} \tag{3}$$

Note that the buckling stress in Equation 2 is a reference stress only and does not rigorously reflect a bifurcation stress in the plate, and a is a multiplier on F_y specific to local buckling effects. A typical observation from experiments is that an element with $F_{cr} \cong 2F_y$ is needed to develop first yield at the extreme fiber in a full section. If the plate buckling coefficient, k, is also assumed, then the coefficient C may be found. These coefficients are tabulated in AISC 360, Table B4.1. For example, for the flange of a rolled shape to develop the plastic moment, AISC 360 provides:

$$\begin{aligned}\lambda_p &= \left(\frac{w}{t}\right)_p \\ &= C\sqrt{\frac{E}{F_y}} \\ &= 0.38\sqrt{\frac{E}{F_y}}\end{aligned} \tag{4}$$

In much of the literature, a related but slightly different approach has been taken to finding coefficients similar to C. A nondimensional slenderness is defined as $\lambda^* = \sqrt{F_y/F_{cr}}$, and this parameter is examined to determine when the objective is met. The two methods are related:

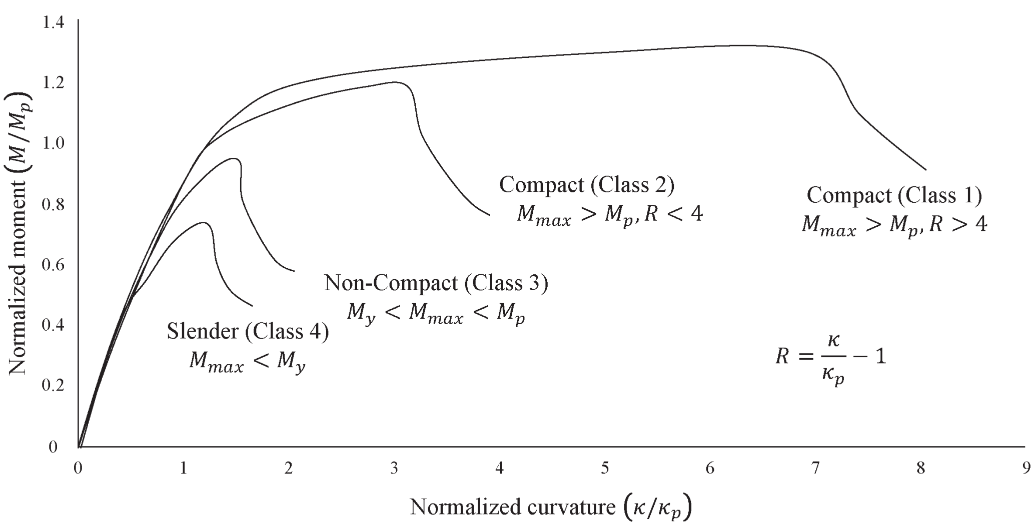

Fig. 1. Moment-curvature behavior of beams with different w/t *limits (based on Wilkinson and Hancock, 1998).*

$$\lambda^* = \sqrt{\frac{F_y}{F_{cr}}} \tag{5}$$
$$= \sqrt{\frac{1}{a}}$$
$$= \sqrt{\frac{12(1-\nu^2)}{k\pi^2 E}}\left(\frac{w}{t}\right)$$

For example, in Winter's classical work (1947), he found that $\lambda^* = 0.673$ or $a = 2.21$ was an accurate boundary between elements that could develop their first yield capacity and those that required additional reductions due to local buckling.

A variety of approaches have been employed to develop *w/t* limits for design. The most common approach is wholly experimental; however, sometimes the experiments have been conducted on idealized elements/plates and sometimes on entire sections. In some cases, researchers directly try to fit their data to the coefficient C of Equation 3, in other cases the focus is on finding the a or λ^* of Equation 2 or 5. Also, in some instances researchers have used Equation 3 in some form to backsolve for k. This can lead to unintended consequences when such k values are reinserted into elastic buckling expressions and used in other settings.

It is worth noting that in developing *w/t* limits, Equation 1 has sometimes been modified to be aligned with the tangent modulus theory and/or application of plasticity reduction factors to the modulus (Ziemian et al., 2010). These approaches can be problematic. Although flexural buckling of columns may be one-dimensional, plate buckling is inherently two-dimensional, and simple one-dimensional reductions to the modulus and ignoring the inherent post-buckling of the plates can lead to erroneous conclusions about strength and *w/t* limits. In several instances, researchers have found it useful to conceptualize Equation 1 in terms of one-dimensional strain instead of stress:

$$\varepsilon_{cr} = \frac{F_{cr}}{E} = k\frac{\pi^2}{12(1-\nu^2)}\left(\frac{t}{w}\right)^2 \tag{6}$$

Equation 6 has the desirable feature of being independent of modulus of elasticity and thus, researchers and specifications in structural thermoplastics or gradual yielding materials (e.g., stainless steel) have often preferred this form. If one follows Equation 6 in establishing *w/t* limits, then instead of determining an F_{cr} in excess of F_y (i.e., aF_y), one thinks in terms of multiples of the yield strain (i.e., $a\varepsilon_y$). This is more natural in inelastic cases, particularly for plastic redistribution or seismic design. It is also worth noting that in the classical literature for developing steel *w/t* limits, it was sometimes common to consider *w/t* limits that achieve a certain average applied strain. A typical target was for the element to sustain a strain up to the initiation of strain hardening, or three or four times the strain at first yield, ε_y. The format of Equation 6 is particularly convenient for such considerations, though one must be careful in that the critical strain is not a direct predictor of the strain that an element can sustain, but rather a parameter that is correlated with the desired strain. See Schafer et al. (2020) for further discussion.

NONSEISMIC AISC 360 LOCAL BUCKLING LIMITS

AISC 360, Section B4, provides local buckling (*w/t*) limits for compression, λ_r, and for flexure, λ_r and λ_p. These limits are utilized to determine domains in which local buckling influences the nominal strength, and those domains are used as primary parameters for establishing strength reductions. A thorough review of AISC 360 local buckling limits is provided herein; however, additional beneficial information is also provided in AISC 360, Section B4.1 Commentary, particularly for round sections that are not covered in detail here.

Objective of AISC 360 Local Buckling Limits

As implemented, the specific objectives of the AISC local buckling limits depend on the loading. For members under axial compression, λ_r provides the slender/nonslender limit for the section; specifically for $w/t \le \lambda_r$, the cross section can develop its squash (yield) strength—that is, $P_y = A_g F_y$. For members under flexure, λ_r provides the noncompact/slender limit for the section; specifically for $w/t \le \lambda_r$ the cross section can develop at least its elastic limit in bending—that is, M_r. In AISC 360, M_r varies by section and limit state and may be defined as $M_r = M_y = SF_y$ or $M_r = SF_L = 0.7M_y$, ostensibly to consider residual stresses. In flexure, λ_p provides the compact/noncompact limit for the section; for $w/t \le \lambda_p$, the cross section can develop its ideal fully plastic capacity in bending—that is, $M_p = ZF_y$.

For members under flexure, the use of either F_y or F_L in determining λ_r creates complications. For Table B4.1b, Case 11 (flanges of I-shaped built-up sections), when $w/t = \lambda_r$, the cross section can develop its first yield capacity considering residual stresses—that is, $M_r = SF_L$, where $F_L = F_y - F_r$ and F_r is the assumed level of residual stress. Other elements (e.g., webs of I-shaped sections) may have implicit consideration of residual stresses in determining λ_r, but do not use F_L in the final width-to-thickness limit [see Schafer et al. (2020) Appendix 1 for further details]. Note, in the 1999 AISC LRFD *Specification* (AISC, 1999), a precursor to AISC 360, the use of $F_L = F_y - F_r$ in the flexural limits was far more pervasive; the following flexural cases used F_L: flanges of rolled I-shapes or channels; flanges of built-up I-shapes; and flanges of HSS, box sections, or cover plates. Also, $F_r = 10$ ksi was used for rolled shapes, and $F_r = 16.5$ ksi was used for welded shapes.

In relation to λ_r, AISC 360, Section B4.1 Commentary, states "Noncompact sections can develop partial yielding in compression elements before local buckling occurs but will not resist inelastic local buckling at the strain levels required for a fully plastic stress distribution. Slender-element sections have one or more compression elements that will buckle elastically before the yield stress is achieved." As currently stated in AISC 360, the noncompact/slender boundary, λ_r, is poorly defined, and interpretation of F_y vs. F_L hinges on interpretation of plate behavior at the boundary between "buckling elastically" and resisting inelastic buckling "but not a full plastic stress." Currently, different cross sections in Chapter F use different approaches to this issue—as discussed later in this paper. In general, the use of F_L relaxes (liberalizes) the w/t limits. A justification given for this application in Salmon et al. (2009) is that this relaxation should be allowed for cases where key residual stresses are tensile in nature.

While λ_p specifically addresses strength, there is some confusion over whether or not it addresses rotation/curvature capacity. For example, see Figure 1, where the term compact refers both to Class 1 and Class 2 sections. AISC 360, Section 1.3.2b Commentary, states that "compact sections … possess a rotation capacity, R_{cap}, of approximately three," where R_{cap} is the rotation at which the post-peak response drops back below M_p normalized by the elastic rotation at which M_p is first reached. In some cases (e.g., Table B4.1b, Cases 17 and 19 for elements of HSS sections), the λ_p limit was specifically selected to meet a minimum R_{cap} of 3. In other cases, as detailed in Appendix 1 of Schafer et al. (2020), there is not a direct connection between a target rotational capacity and the selected w/t limit, or the target rotational capacity was not 3. However, in available experiments on I-shaped beams that meet the λ_p criteria, all sections develop at least an R_{cap} of 2.9, and in many cases far in excess of this (Schafer et al., 2020). The AISC 360 λ_p limits provide strength M_p and also supply a level of strain capacity in the element in excess of the yield strain. In many instances, researchers targeted a strain capacity up to the onset of strain hardening in the material [see Appendix 1 of Schafer et al. (2020) and AISC 341, Section D1.1b Commentary]. The end result of these varied approaches is that the section typically can sustain a rotation capacity of approximately 3 or more. One notable exception is Table B4.1b, Case 14: tee-stems in Chapter F of AISC 360, λ_p is associated with the first yield moment, M_y, instead of the fully plastic moment, M_p.

Comparison with Eurocode

Provided in this paper is a comparison of the local buckling limits between AISC 360 and Eurocode EN 1993-1-1 (CEN, 2004). Additional comparisons to ANSI/AISI S100-16, *North American Specification for the Design of Cold-Formed Steel Structural Members* (2016), herein referred to as AISI S100; the 8th Edition of the AASHTO *LRFD Bridge Design Specification* (AASHTO, 2017); and *Recommendations for Limit State Design of Steel Structures* from the Architectural Institute of Japan (AIJ, 2010), herein referred to as AIJ, are provided in Schafer et al. (2020). Due to its similar design rules with respect to local buckling and maturity with respect to application, direct comparison of AISC 360 w/t limits to those of Eurocode is desirable. Table 5.2 in Part 1-1 of Eurocode 3 is the counterpart to AISC 360, Table B4.1. However, the format for presenting the limits is not identical. For a typical w/t limit, Eurocode expresses the limit as:

$$\left(\frac{w}{t}\right)_{limit} \le C_{EN}\sqrt{\frac{235}{F_{yMPa}}} \tag{7}$$

where F_{yMPa} indicates the yield stress in units of MPa, and C_{EN} is a nondimensional coefficient provided in Eurocode. For a direct comparison with AISC's format of $C\sqrt{E/F_y}$, the equivalent C coefficient in AISC's format may be found from:

$$C_{eq} = C_{EN}\sqrt{\frac{235}{E_{MPa}}} \text{ or } 0.0343C_{EN} \tag{8}$$

where E_{MPa} indicates the modulus of steel in MPa. Comparison for compression is provided in Table 1 and for flexure in Table 2, wherein cases with substantial differences are highlighted in gray within the tables.

For compression members, AISC stiffened element w/t limits are quite similar to Eurocode. However, AISC unstiffened element w/t limits are different from Eurocode; for example, the AISC w/t limit is 36% higher than Eurocode for the stem of a tee section. For flexural members, AISC and Eurocode have greater differences. In flexure, AISC w/t limits are generally similar to Eurocode for stiffened elements but dissimilar, sometimes significantly, for unstiffened elements. AISC's unstiffened element flange λ_p limit is greater than even Class 2 for Eurocode, which implies that Eurocode would not predict even minimal rotational capacity for members with flanges at the AISC λ_p limit. The AISC λ_r limit for unstiffened elements is more than double Eurocode Class 3, even for the simple case of a rolled flange.

Additional differences related to w/t limits between the standards also exist. AISC differentiates between rolled and built-up shapes, while Eurocode does not. AISC includes web-flange interaction for flanges of built-up shapes, while Eurocode does not. Note that AISC differentiates between compression and flexural members when defining the w/t limits; Eurocode does not. Instead, Eurocode considers the assumed stress on an element more explicitly than AISC. Thus, Eurocode provides w/t limits that consider arbitrary compression and bending. In minor-axis bending of

Table 1. AISC 360 *w/t* Limits for Compression Elements in Members Subject to Axial Compression and Eurocode *w/t* Limits for Elements in Uniform Compression			
	Element Description	**AISC 360**	**Eurocode**
Case	**Unstiffened**	λ_r	**Class 3**
1	Rolled flange	$0.56\sqrt{\frac{E}{F_y}}$	$0.48\sqrt{\frac{E}{F_y}}$
2	Built-up flange	$0.38 \text{ to } 0.56\sqrt{\frac{E}{F_y}}$ [a]	$0.48\sqrt{\frac{E}{F_y}}$
3	Angle leg, other	$0.45\sqrt{\frac{E}{F_y}}$	$0.51\sqrt{\frac{E}{F_y}}$
4	Stem of tee	$0.75\sqrt{\frac{E}{F_y}}$	$0.48\sqrt{\frac{E}{F_y}}$
	Stiffened		
5	Rolled web	$1.49\sqrt{\frac{E}{F_y}}$	$1.44\sqrt{\frac{E}{F_y}}$
6	HSS wall	$1.40\sqrt{\frac{E}{F_y}}$	$1.44\sqrt{\frac{E}{F_y}}$
7	Cover plate	$1.40\sqrt{\frac{E}{F_y}}$	$1.44\sqrt{\frac{E}{F_y}}$
8	Other	$1.49\sqrt{\frac{E}{F_y}}$	$1.44\sqrt{\frac{E}{F_y}}$
	Round		
9	Round HSS/pipe	$0.11\sqrt{\frac{E}{F_y}}$	$0.11\sqrt{\frac{E}{F_y}}$

[a] AISC provisions are a function of web h/t_w, bounds provided here, shading highlights substantial differences.

unstiffened elements, for example, considering the stress distribution explicitly as Eurocode does can lead to stark differences depending on whether or not the tip of the unstiffened element is in tension or compression. Generally, Eurocode's *w/t* limits are more closely aligned with the underlying assumptions of the effective width method as, for example, implemented in AISI S100 (2016).

Plate Buckling Assumptions Implied in AISC 360 *w/t* Limits

If one considers a given *w/t* limit expressed by the coefficient C of Equation 3, this coefficient is directly connected to (1) the assumed plate buckling coefficient, k (i.e., the loading and boundary conditions of the plate), and (2) the plate slenderness, λ^*, required to sustain the desired load or stress/strain. Combining Equation 3 and 5 at the λ_r for pure compression results in:

$$\begin{aligned}\lambda_r &= \left(\frac{w}{t}\right)_r \\ &= \lambda^* \sqrt{\frac{k\pi^2}{12(1-\nu^2)}}\sqrt{\frac{E}{F_y}} \\ &= C\sqrt{\frac{E}{F_y}}\end{aligned} \tag{9}$$

The most complete discussion of the underlying assumptions for the AISC 360 *w/t* limits can be found in Salmon et al. (2009). For the λ_r limits of compression members, Salmon et al. provide most of the assumed λ^* and plate buckling coefficients, k. With these assumed values, Table 3 shows that the resulting λ_r limits match AISC 360.

Examination of the assumed k and λ^* values based on Equation 9 for flexure are more complex. Nonetheless, it can be completed with some success and is provided for

Table 2. AISC 360 w/t Limits for Compression Elements in Flexural Members and Eurocode w/t Limits for Elements with Compressive Stress						
	Element Description	**AISC 360**	**Eurocode**	**Eurocode**	**AISC 360**	**Eurocode**
Case	**Unstiffened**	λ_p	**Class 1**	**Class 2**	λ_r	**Class 3**
10	Rolled flange	$0.38\sqrt{\frac{E}{F_y}}$	$0.31\sqrt{\frac{E}{F_y}}$	$0.34\sqrt{\frac{E}{F_y}}$	$1.0\sqrt{\frac{E}{F_y}}$	$0.48\sqrt{\frac{E}{F_y}}$
11	Built-up flange[a]	$0.38\sqrt{\frac{E}{F_y}}$	$0.31\sqrt{\frac{E}{F_y}}$	$0.34\sqrt{\frac{E}{F_y}}$	$0.56 \text{ to } 0.83\sqrt{\frac{E}{F_y}}$	$0.48\sqrt{\frac{E}{F_y}}$
12	Angle leg, other	$0.54\sqrt{\frac{E}{F_y}}$	$0.31\sqrt{\frac{E}{F_y}}$	$0.34\sqrt{\frac{E}{F_y}}$	$0.91\sqrt{\frac{E}{F_y}}$	$0.48\sqrt{\frac{E}{F_y}}$
13	Flange in minor axis[b]	$0.38\sqrt{\frac{E}{F_y}}$	$0.31 \text{ to } 0.63\sqrt{\frac{E}{F_y}}$ $0.31 \text{ to } 0.93\sqrt{\frac{E}{F_y}}$	$0.34 \text{ to } 0.68\sqrt{\frac{E}{F_y}}$ $0.34 \text{ to } 1.02\sqrt{\frac{E}{F_y}}$	$1.0\sqrt{\frac{E}{F_y}}$	$0.48 \text{ to } 1.44\sqrt{\frac{E}{F_y}}$
14	Stem of tee[b]	$0.84\sqrt{\frac{E}{F_y}}$	$0.31 \text{ to } 0.62\sqrt{\frac{E}{F_y}}$ $0.31 \text{ to } 0.93\sqrt{\frac{E}{F_y}}$	$0.34 \text{ to } 0.68\sqrt{\frac{E}{F_y}}$ $0.34 \text{ to } 1.02\sqrt{\frac{E}{F_y}}$	$1.52\sqrt{\frac{E}{F_y}}$	$0.48 \text{ to } 1.44\sqrt{\frac{E}{F_y}}$
	Stiffened					
15	Web (doubly symmetrical shape)	$3.76\sqrt{\frac{E}{F_y}}$	$2.46\sqrt{\frac{E}{F_y}}$	$2.84\sqrt{\frac{E}{F_y}}$	$5.70\sqrt{\frac{E}{F_y}}$	$4.25\sqrt{\frac{E}{F_y}}$
19	Web HSS and box	$2.42\sqrt{\frac{E}{F_y}}$	$2.46\sqrt{\frac{E}{F_y}}$	$2.84\sqrt{\frac{E}{F_y}}$	$5.70\sqrt{\frac{E}{F_y}}$	$4.25\sqrt{\frac{E}{F_y}}$
16	Web (singly symmetrical shape)	c	c	c	$5.70\sqrt{\frac{E}{F_y}}$	c
17	Flange HSS	$1.12\sqrt{\frac{E}{F_y}}$	$1.13\sqrt{\frac{E}{F_y}}$	$1.65\sqrt{\frac{E}{F_y}}$	$1.40\sqrt{\frac{E}{F_y}}$	$1.44\sqrt{\frac{E}{F_y}}$
18	Flange cover plate	$1.12\sqrt{\frac{E}{F_y}}$	$1.13\sqrt{\frac{E}{F_y}}$	$1.65\sqrt{\frac{E}{F_y}}$	$1.40\sqrt{\frac{E}{F_y}}$	$1.44\sqrt{\frac{E}{F_y}}$
21	Flange box sections	$1.12\sqrt{\frac{E}{F_y}}$	$1.13\sqrt{\frac{E}{F_y}}$	$1.65\sqrt{\frac{E}{F_y}}$	$1.49\sqrt{\frac{E}{F_y}}$	$1.44\sqrt{\frac{E}{F_y}}$
	Round					
20	Round HSS/ pipe	$0.07\sqrt{\frac{E}{F_y}}$	$0.06\sqrt{\frac{E}{F_y}}$	$0.08\sqrt{\frac{E}{F_y}}$	$0.31\sqrt{\frac{E}{F_y}}$	$0.11\sqrt{\frac{E}{F_y}}$

[a] AISC provisions are a function of web h/t_w, bounds provided here, $F_L = 0.7F_y$.
[b] Eurocode provisions provide limit as a function of whether unsupported tip is in compression or tension and specific to the plastic or elastic stress distribution on the unstiffened element. Typical ranges provided here.
[c] AISC provisions are a function of ENA to PNA distances, Eurocode provisions a function of PNA for Class 1 and Class 2, ENA for Class 3—i.e., stress gradient dependent, shading highlights substantial differences.

Table 3. Assumptions Underlying AISC 360 w/t Limits—λ_r Compression Elements in Members Subject to Axial Compression Only					
	Element Description	k	$\lambda^* = \sqrt{\frac{F_y}{F_{cr}}}$	Equation 10	AISC 360
Case	**Unstiffened**			λ_r	λ_r
1	Rolled flange	0.70[a]	0.70[f]	$0.56\sqrt{\frac{E}{F_y}}$	$0.56\sqrt{\frac{E}{F_y}}$
2	Built-up flange	0.35 ~ 0.76	0.70[f]	$0.39 \text{ to } 0.58\sqrt{\frac{E}{F_y}}$	$0.38 \text{ to } 0.56\sqrt{\frac{E}{F_y}}$
3	Angle leg, other	0.425[b]	0.70[f]	$0.43\sqrt{\frac{E}{F_y}}$	$0.45\sqrt{\frac{E}{F_y}}$
4	Stem of tee	1.277[c]	0.70[f]	$0.75\sqrt{\frac{E}{F_y}}$	$0.75\sqrt{\frac{E}{F_y}}$
	Stiffened				
5	Rolled web	5.0[d]	0.70[f]	$1.49\sqrt{\frac{E}{F_y}}$	$1.49\sqrt{\frac{E}{F_y}}$
6	HSS wall	4.4[e]	0.70[f]	$1.40\sqrt{\frac{E}{F_y}}$	$1.40\sqrt{\frac{E}{F_y}}$
7	Cover plate	4.4[e]	0.70[f]	$1.40\sqrt{\frac{E}{F_y}}$	$1.40\sqrt{\frac{E}{F_y}}$
8	Other	5.0[d]	0.70[f]	$1.49\sqrt{\frac{E}{F_y}}$	$1.49\sqrt{\frac{E}{F_y}}$

[a] Approximately halfway between pinned and fixed k values.
[b] Ideal case for simple-free longitudinal edge conditions.
[c] Ideal case for fixed-free longitudinal edge condition.
[d] Approximately one-third of the way between pinned and fixed k values.
[e] This k factor back-calculated from λ^* and the w/t limit.
[f] Nondimensional slenderness to achieve a plate strength approaching F_y.

the λ_r and λ_p limits in Table 4. Completion of this effort reveals some key assumptions embedded within the current AISC 360 w/t limits. It is important to note, particularly for the λ_p limits, that the plastic strength limits are usually not derived on the basis of Equation 9 or similar; rather, they are determined experimentally. Here we are able to observe after the fact if simple unifying methods/assumptions still exist despite the largely experimental basis.

For all elements of compression members, $\lambda_r^* = \sqrt{F_y/F_{cr}} = 0.7$, implying $F_{cr} \cong 2F_y$ is necessary for an element to reach its yield stress. This is predicated upon assumptions about the plate bucking coefficient, k, but is consistent across the w/t limits. AISC 360 assumes singular k values and ignores element interaction (in all but one case). Selected k values are generally between simply supported and fixed edge boundary conditions, except for stems of tees which use the maximum fully fixed edge condition assumption. For flexural members, the assumptions are far more complicated, with many exceptions. In the following, sections, both λ_r and λ_p for flexure are discussed.

Further Examination of λ_r Limits in Flexure

Overall, the plate buckling coefficient k values for λ_r in flexure (Table 4) follow the same logic as for compression members; however, providing definitive background reasoning for some cases is hard to finalize—for example, Case 10 for a rolled flange using $k = 0.7$ and $\lambda_r^* = 1.0$ still results in a more conservative w/t limit than specified in AISC 360, potentially due to F_L in past use ($k = 1.1$ provides agreement with AISC 360). For λ_r in flexural members, Table 4 shows that AISC 360 generally employs $\lambda_r^* = 1.0$, implying $F_{cr} = F_y$ is all that is necessary for an element to reach its target stress (i.e., F_y or F_L) at the extreme compression fiber. This is more liberal than $\lambda_r^* = 0.7$ used for

Table 4. Assumptions Underlying AISC 360 w/t Limits—λ_r and λ_p
Compression Elements in Members Subject to Flexure

	Element Description	k	$\lambda_p^* = \sqrt{\frac{F_y}{F_{cr}}}$	Equation 10	AISC 360	k	$\lambda_r^* = \sqrt{\frac{F_y}{F_{cr}}}$	Equation 10	AISC 360
Case	**Unstiffened**			λ_p	λ_p			λ_r	λ_r
10	Rolled flange	0.7[a]	0.464[h]	$0.37\sqrt{\frac{E}{F_y}}$	$0.38\sqrt{\frac{E}{F_y}}$	0.7[a]	1.0[m]	$0.80\sqrt{\frac{E}{F_y}}$	$1.00\sqrt{\frac{E}{F_y}}$
11	Built-up flange	0.35 to 0.76[b]	0.464[h]	$0.26 \text{ to } 0.38\sqrt{\frac{E}{F_y}}$	$0.38\sqrt{\frac{E}{F_y}}$	0.35 to 0.76[b]	1.0[n]	$0.56 \text{ to } 0.83\sqrt{\frac{E}{F_y}}$	$0.56 \text{ to } 0.83\sqrt{\frac{E}{F_y}}$
12	Angle leg	0.90[c]	0.464[h]	$0.42\sqrt{\frac{E}{F_y}}$	$0.54\sqrt{\frac{E}{F_y}}$	0.90[c]	1.0[m]	$0.90\sqrt{\frac{E}{F_y}}$	$0.91\sqrt{\frac{E}{F_y}}$
13	Flange in minor axis	0.7[a]	0.464[h]	$0.37\sqrt{\frac{E}{F_y}}$	$0.38\sqrt{\frac{E}{F_y}}$	1.1[c]	1.0[m]	$1.00\sqrt{\frac{E}{F_y}}$	$1.00\sqrt{\frac{E}{F_y}}$
14	Stem of tee (flexure)	2.6[c]	0.464[h]	$0.71\sqrt{\frac{E}{F_y}}$	$0.84\sqrt{\frac{E}{F_y}}$	2.6[c]	1.0[m]	$1.53\sqrt{\frac{E}{F_y}}$	$1.52\sqrt{\frac{E}{F_y}}$
	Stiffened								
15	Web (doubly symmetrical)	36[d]	0.56[i]	$3.19\sqrt{\frac{E}{F_y}}$	$3.76\sqrt{\frac{E}{F_y}}$	36[k]	1.0[o]	$5.70\sqrt{\frac{E}{F_y}}$	$5.70\sqrt{\frac{E}{F_y}}$
19	Web of HSS and box	36[d]	0.56[i]	$3.19\sqrt{\frac{E}{F_y}}$	$2.42\sqrt{\frac{E}{F_y}}$	36[k]	1.0[o]	$5.70\sqrt{\frac{E}{F_y}}$	$5.70\sqrt{\frac{E}{F_y}}$
16	Web (singly symmetrical)	36[e]	0.56[i]	$3.19\sqrt{\frac{E}{F_y}}$[j]	$3.76\sqrt{\frac{E}{F_y}}$[j]	36[l]	1.0[o]	$5.70\sqrt{\frac{E}{F_y}}$	$5.70\sqrt{\frac{E}{F_y}}$
17	Flange of HSS	4.4[f]	0.56[i]	$1.12\sqrt{\frac{E}{F_y}}$	$1.12\sqrt{\frac{E}{F_y}}$	4.4[f]	0.7[p]	$1.40\sqrt{\frac{E}{F_y}}$	$1.40\sqrt{\frac{E}{F_y}}$
18	Flange cover plate	4.4[f]	0.56[i]	$1.12\sqrt{\frac{E}{F_y}}$	$1.12\sqrt{\frac{E}{F_y}}$	4.4[f]	0.7[p]	$1.40\sqrt{\frac{E}{F_y}}$	$1.40\sqrt{\frac{E}{F_y}}$
21	Flange of box	5.0[g]	0.56[i]	$1.19\sqrt{\frac{E}{F_y}}$	$1.12\sqrt{\frac{E}{F_y}}$	5.0[g]	0.7[p]	$1.49\sqrt{\frac{E}{F_y}}$	$1.49\sqrt{\frac{E}{F_y}}$

[a] Estimated as halfway between pinned and fixed k values.
[b] Factor at the limits of expression provided in AISC 360: $k = 0.35 < 4/\sqrt{h/t_w} < 0.76$.
[c] Back-calculated from assumed flexure $\lambda_r^* = 1.0$.
[d] Based on elastic stress distribution, if plastic stress distribution used $k_{pinned} = 10.3$, $k_{fixed} = 15.4$, $k_{80\%} = 14.4$ (also see note k).
[e] Based on bending about symmetry axis, but k would be a function of ENA location in reality.
[f] Back-calculated from compression λ^* and w/t limit, same in flexure as compression.
[g] Estimated as one-third of the way between pinned and fixed k values for pure compression.
[h] 0.46 based on Haaijer and Thurlimann (1960) as onset of strain hardening in unstiffened element, also connects to continuous strength method (CSM) base curve by Gardner et al. (2019) and implies $4\varepsilon_y$ at this slenderness.
[i] 0.56 based on Haaijer and Thurlimann (1960) as onset of strain hardening in unstiffened element, also connects to CSM base curve by Gardner et al. (2019) and implies $2\varepsilon_y$ at this slenderness.
[j] Expression varies, value here for ENA = PNA and $M_p/M_y = 1.12$ (typical rolled shape I); i.e., the symmetrical limit.
[k] Based on symmetrical bending, 80% of difference from $k_{pinned} = 23.9$ and $k_{fixed} = 39.6$ per Salmon et al. (2009).
[l] Based on bending about symmetry axis, but k would be a function of ENA in reality.
[m] $F_{cr} = F_y$ assumed for λ_r^* because of agreement for Case 11 footnote n; Cases 15, 16, and 19 footnote o; and that even fully fixed values for k are not high enough to give AISC slenderness limits with $\lambda_r^* = 0.7$ as was done in compression.
[n] Built-up flanges assumed to use $F_{cr} = F_y$ for λ_r^*, also see footnote o.
[o] For flexure, AISC 360 assumes $F_{cr} = F_y$ sufficient for extreme fiber of web to reach F_y (Salmon et al., 2009).
[p] For stiffened element flanges, AISC uses same normalized slenderness criteria as for compression members.

Table 5. Application of λ_r Limits for Compression Elements in Members Subject to Flexure in AISC 360, Chapter F							
Section	**Cross Section**	**Element**	**Limit State**	**λ**	**M_r**	**Equation Note**	**Table B4.1b Case**
F3	I-doubly symmetrical	Unstiffened	FLB	λ_{rf}	$0.7M_y$	Explicit in Eq. F3-1	10
F4	I-singly symmetrical	Unstiffened	FLB	λ_{rf}	$0.7M_y$	Or lower per S_{xt}/S_{xc}	10, 11
F5	I	Unstiffened	FLB	λ_{rf}	$0.7M_y$	Explicit in Eq. F5-8	10, 11
F10	L	Unstiffened	LB	λ_r	$0.86M_y$	Implicit in Eq. F10-6	12
F6	I, C, minor	Unstiffened	FLB	λ_{rf}	$0.7M_y$	Explicit in Eq. F6-2	13
F9	Tee, 2L	Unstiffened	FLB	λ_{rf}	$0.7M_y$	Explicit in Eq. F9-14	10
F9	Tee, 2L	Unstiffened	LB flexure	λ_r	$0.65M_y$	Implicit in Eq. F9-18	14
F5	I	Stiffened	WLB	λ_{rw}	M_y	Implicit in R_{pg} per Eq. F5-6	15, 16
F5	I	Stiffened	WLB-LTB	λ_{rw}	M_y	Implicit in R_{pg} per Eq. F5-6	15, 16
F7	Box, HSS	Stiffened	FLB	λ_{rf}	M_y	Implicit in Eq. F7-2	17, 21
F7	Box, HSS	Stiffened	WLB	λ_{rw}	M_y	Implicit in Eq. F7-6	19
F7	Box, HSS	Stiffened	WLB-LTB	λ_{rw}	M_y	Implicit in R_{pg} per Eq. F5-6	19
Note: Subscript *f* or *w* on λ_r refers to flange or web, respectively.							

elements in compression members (implying $F_{cr} \cong 2F_y$). AISC 360 extends this more liberal $\lambda_r^* = 1.0$ to unstiffened element flanges that are part of a flexural member; but *does not* extend this more liberal λ_r^* to stiffened element flanges; these elements use the same λ_r^* as in compression. The use of the more liberal $\lambda_r^* = 1.0$ appears to originate in past practice for plate girder design. Note that other studied specifications—Eurocode, AISI S100, and AIJ—do not make this assumption, leading to fairly stark differences between slender element w/t limits of flexural members.

Hidden in these comparisons are the past use of F_L, which liberalizes the w/t limit, and whether or not the limit is intended to achieve an M_r of M_y or $0.7M_y$. A review of the application of λ_r in AISC 360, Chapter F, is provided in Table 5. The λ_r for unstiffened elements provides an M_r of $0.7M_y$, while for stiffened elements in flexure, λ_r intends to establish an M_r of M_y. As detailed in Table 5, the connection is explicit for some cases, while in other cases, substitution of appropriate λ_r values must be completed to determine the strength that $\lambda = \lambda_r$ implies.

The use of λ_r for flanges must be understood in the context of the strength predictions of AISC 360, Chapter F. For the prototypical flange local buckling (FLB) case, Figure 2 illustrates the solution. It can be observed that λ_r is an anchor point in the strength prediction and is typically tied to $M_r = 0.7M_y$. While it is true that AISC 360 transitions to the plate elastic buckling curve for $\lambda > \lambda_r$, actual behavior does not have a sharp inelastic/elastic transition. Thus, λ_r is not at a definitive transition to elastic stress, but rather is an anchor point in a strength curve deemed to provide reasonable cross-section flexural strength prediction. Note that Eurocode and AISI S100 follow Winter's equation (Winter, 1947) anchored to M_y instead of $0.7M_y$ and include post-buckling. Thus, the particulars of the strength curves selected in AISC 360, Chapter F (particularly M_r) end up influencing the consistency of the λ_r limits in Chapter B.

The use of λ_r for webs in Chapter F is primarily handled through the R_{pg} reduction factor. Note that the connection between web slenderness limits and bending strength is particularly indirect and strongly dependent on the flange because the flange contributes much more to cross-section moment of inertia, I, and plastic section modulus, Z, than the web. Thus, a large error in a web slenderness limit may have only a small impact on the flexural strength prediction of many common sections. Nonetheless, the use of $\lambda_r^* = 1.0$ for the $M_r = M_y$ cases (15, 16, and 19) is difficult to justify based on plate mechanics arguments.

Further Examination of λ_p Limits in Flexure

The origin of the flexural compactness limit λ_p may be primarily understood as being derived from limits on the nondimensional slenderness λ_p^*. Historically, this has been based on mechanical approximations, setting $\lambda_p^* \cong 0.46$ for unstiffened elements and $\lambda_p^* \cong 0.58$ for stiffened elements (Haaijer and Thurlimann, 1960). Today, based on the work of Gardner and colleagues (e.g., Afshan and Gardner, 2013; Zhao et al., 2017), this could be characterized as providing $4\varepsilon_y$ for unstiffened elements and $2\varepsilon_y$ for stiffened elements. Unstiffened element λ_p generally follows $\lambda_p^* \cong 0.46$; however, Case 12 (legs of single angles in Table 4) has a more relaxed λ_p limit than Case 10 (flanges of rolled shapes).

Because Case 12 includes the possibility of the angle leg bent about a geometric axis that places the entire element in compression (essentially the same as Case 10), the origin of the difference is not entirely clear. A possible reason is the application of upper bounds on M_p in AISC 360. For example, for an angle section, M_p is limited to $1.5M_y$, even though the typical shape factor is 1.8; therefore, the λ_p required to reach $1.5M_y$ may be more relaxed than that to reach M_p.

Stiffened element λ_p, when the element is in compression, is generally consistent with the overall practice regarding a limiting $\lambda_p^* \cong 0.56$; this is true even for HSS where the limit was derived experimentally on full sections without direct consideration of the underlying assumptions (Wilkinson and Hancock, 1998). Stiffened element λ_p, when the element is in flexure, does not agree particularly well with the overall assumption of slenderness $\lambda_p^* \cong 0.56$. Further, if the k is based on the plastic, not the elastic, stress distribution, k would be considerably lower, leading to an even larger disagreement between assumed and actual λ_p in AISC 360 for stiffened elements in flexure.

Discussion of Local Buckling Web-Flange Interaction

Web-flange interaction is shorthand for the phenomenon that the isolated plate solutions that are typically used to predict local buckling are not actually isolated but, instead, interact. Equilibrium and compatibility are, of course, maintained between elements in a cross section when undergoing elastic or inelastic local buckling. In this regard, the separation into flange local buckling (FLB) and web local buckling (WLB) is artificial—the web and flange of cross sections always interact. The primary question is this: To what extent does this interaction matter? The traditional conclusion, for rolled shapes at yield stresses consistent with mild steel, is that the interaction is either weak or otherwise does not vary much and can be approximated for standard (rolled) shapes by treating FLB and WLB as essentially constant and separate plate phenomena. This assumption is largely embedded in the w/t limits in AISC 360.

For nonseismic w/t limits, the one case where web-flange interaction is explicitly considered in AISC 360 is in the w/t limits for flanges of built-up I-shapes. For this case, k is calculated with the assumption:

$$k = 0.35 < \frac{4}{\sqrt{h/t_w}} < 0.76 \tag{10}$$

Equation 10 is a simplification of the expression provided by Johnson (1976), where k was approximated from testing employing the basic mechanics outlined in Haaijer and Thurlimann (1960). Notably, this k is not a plate buckling coefficient in the traditional sense and does not agree well with elastic theory. A comparison was made employing the expressions in Seif and Schafer (2010), and Equation 10 is higher than the elastic solution. However, White (2008) found that the expression, albeit a simplification, works generally well with available data from a strength perspective.

Web-flange interaction is implicitly considered for other elements in the AISC w/t limits, but at assumed levels of rigidity as detailed in the footnotes to Table 3 and Table 4. For example, the k for an I-section flange in a compression member is assumed to be 0.7, which is halfway between the rigidity limits of a simply supported and a fixed longitudinal edge. This sounds rational, but when compared to the actual elastic k based on thin-plate theory and including web-flange interaction for I-sections [Figure 3(b)] in compression, this k is quite optimistic (Seif and Schafer, 2010).

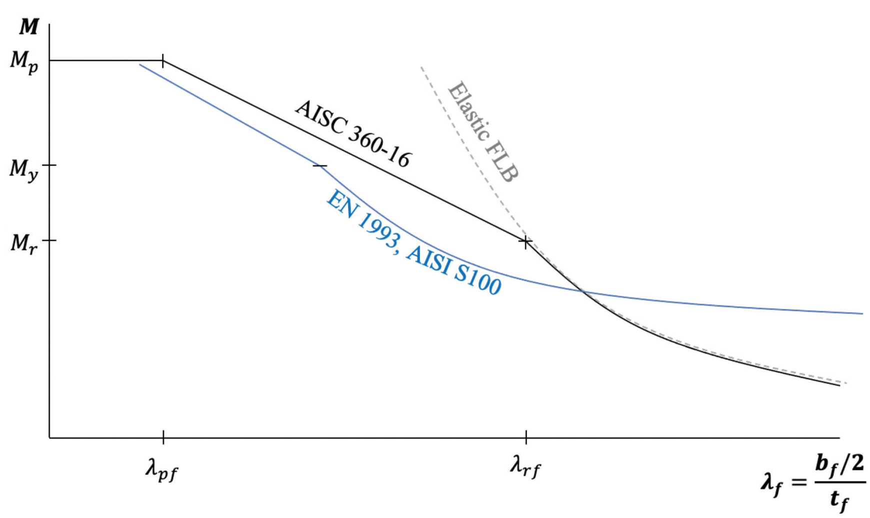

Fig. 2. Typical application of λ_r in flange local buckling for AISC 360 compared with other standards.

The compressive stress on the web degrades the flange plate buckling coefficient, k. This is not uncommon because it is not just the rigidity, but also the stress on the attached elements that influences the local cross-section stability. In flexure, the web stability is significantly enhanced from the compression case, and the mean flange k for I-sections is as high as 1.2 [Figure 3(a)] and compares favorably with the back-calculated k from AISC's flexural λ_r limit. The footnotes of Table 3 and Table 4 specifically address the k value and their implicit assumptions about web-flange interaction for all w/t cases; comparisons are provided for nearly all cases in Seif and Schafer (2010). It is recommended in Seif and Schafer that mean k values (determined from elastic buckling of all relevant rolled shapes) or values based on a given exceedance probability be selected so as to provide uniformity across elements even if a single k is selected. This is a reasonable suggestion, but it would lead to changes in almost all λ_r limits in AISC 360. Alternatives are explored later in this paper.

The dependency of the plate buckling coefficient on the applied stress leads to another important consideration in web-flange interaction: how to handle w/t limits for beam-columns. Earlier editions of the AISC *Specification*—for example, the first edition of the AISC LRFD *Specification* (1986)—included w/t limits for "webs in combined flexure and axial compression" that were a function of the stress gradient captured through the ratio of P_r/P_y, where P_r is the required axial strength and P_y is the squash load. These provisions were later simplified using the compression w/t limit throughout; however, AISC 341 has maintained a dependence on the compression load that has seen recent study as discussed in Section 4.3. See Schafer et al. (2020) for additional discussion on implementing stress-dependent w/t limits for beam-columns in AISC 360.

Analytical expressions, derived from simulations, are available to provide closed-formed solutions for accurate plate buckling coefficients, k, or, more directly, the cross-section local buckling load, $P_{cr\ell}$, or moment, $M_{cr\ell}$. Seif and Schafer (2010) provide one set of solutions, and Fieber et al. (2019) have recently derived another set. In addition, efficient and simple computational programs exist for calculating cross-section local buckling [see Appendix 2 of AISI S100 (2016) for extensive commentary, including links to software] and all buckling values for common shapes could be tabulated in much the same way as complex section properties such as C_w are tabulated for use in design.

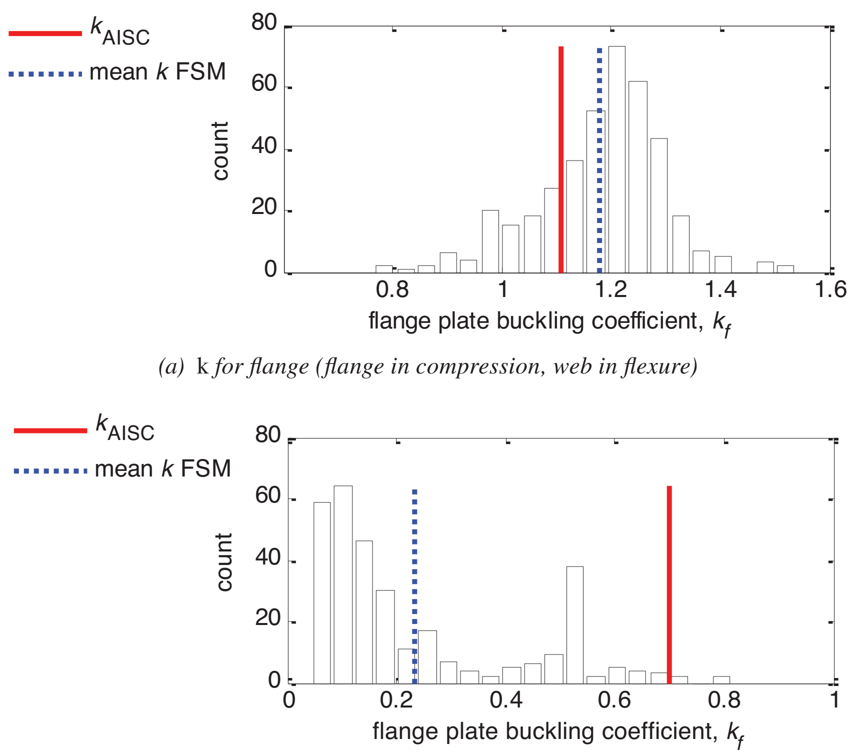

(a) k for flange (flange in compression, web in flexure)

(b) k for flange (flange in compression, web in compression)

Fig. 3. Excerpt from Seif and Schafer (2010). Example of flange buckling k_f *for all I-sections in AISC* Manual *(a) flexure and (b) compression compared with* k *assumed in* w/t *development.*

AISC 341 LOCAL BUCKLING LIMITS FOR SEISMIC DESIGN

Since their introduction in 1990 in the AISC *Seismic Provisions* (AISC, 1990), the local buckling (i.e., w/t) requirements have undergone regular revision. The seismic w/t limits are part of the ductility design requirements to ensure adequate inelastic deformation capacities. The requirements in the 1990 edition of the *Seismic Provisions* were basically those from the 1988 Uniform Building Code (ICBO, 1988), which were based on limited research conducted in the 1970s and 1980s. The seismic local buckling requirements were also strongly influenced by the plastic design provisions in the AISC *Specification*.

The Northridge Earthquake in 1994 triggered a new wave of seismic steel research activities, not only for special moment frames (SMFs) but also for other types of seismic force-resisting systems (SFRSs). AISC 341, Table D1.1, provides the limiting w/t ratios for all SFRS covered in AISC 341 (see Table 6). Starting with the 2010 edition of AISC 341, this table expresses local buckling requirements in the form of λ_{hd} values for highly ductile members and λ_{md} values for moderately ductile members in lieu of the previously used terms: seismically compact and compact. This change in terminology was made because the limiting w/t ratios did not always reflect limit states consistent with the AISC 360 use of "compact." Up until 2010, the limiting λ values were written as a function of E and F_y, but starting in 2016, these formulae were converted to a new format by replacing the nominal yield stress, F_y, by the expected yield stress, R_yF_y, and changing the coefficients under assumed R_y values as discussed in Section 4.2.

Objectives

Local bucking, w/t, limits in AISC 341 serve multiple objectives, and their application is typically dependent on the SFRS. AISC 341, Table D1.1, provides two limits: moderately ductile λ_{md} and highly ductile λ_{hd}; however, the limits are not only a function of the type of element in a section (e.g., stiffened vs. unstiffened), but also a function of how the section is employed in the SFRS. For example, a diagonal brace in a special concentrically braced frame (SCBF) and in an eccentrically braced frame (EBF) are treated differently, as is a beam in a SMF versus in a buckling-restrained braced frame (BRBF). Focusing on I-shaped beams in intermediate moment frames (IMFs) and SMFs as the prototypical application of local buckling w/t limits, the AISC 341 Commentary provides the basic objectives: λ_{md} provides a section that can undergo plastic rotation of 0.02 rad or less, and λ_{hd} provides a section that can undergo plastic rotation of 0.04 rad or more. The Commentary further states that λ_{md} in AISC 341 is generally the same as λ_p in AISC 360, with the exception of HSS, stems of WTs, and webs in flexure. Further, λ_{hd} is typically stricter than λ_p, though in several cases this is relaxed. A summary of all current w/t limits for AISC 360 and AISC 341 is provided in Table 6.

To fully understand the objective in the application of the λ_{md} and λ_{hd} limits, one must go through each SFRS. A summary of the application of these limits and their intended objective is provided in Table 7 and complete details are provided in Schafer et al. (2020). In general, the following observations can be made regarding the objectives of λ_{md} and λ_{hd}:

- λ_{md}: Provide enough ductility so that the SFRS can develop its system strength, R_r, and last several cycles at that strength (n cycles); provide sufficient compactness so that a member can develop M_p or, in some cases, M_p and at least 0.02 rad, or M_p up to and including strain hardening, M_{pe}. Application of these objectives is system dependent.
- λ_{hd}: Provide enough ductility so that the SFRS can develop its system strength, R_r, and last several system cycles at that strength (n cycles) or system interstory drift (3% ID); provide sufficient compactness so that a member can develop M_p or, in some cases, M_p and at least 0.04 rad rotation (i.e., story drift angle) at a post-peak of $0.8M_p$, or M_p up to and including strain hardening, M_{pe}, or high component level strains ($10–20\varepsilon_y$) and high numbers of component cycles (n cycles). Application of these objectives is system dependent.

When a concern exists regarding seismic behavior of a member, but limited research or knowledge is available, it is common to require λ_{md} or λ_{hd} even if it is not strictly needed for strength. As a result, the objectives for these criteria are sometimes clear and discrete, but more often manifold and complex.

Expected Material Properties and w/t Limits

The use of R_yF_y in AISC 341 and F_y in AISC 360 for the w/t limits creates a discrepancy for the user that requires attention and explanation. If it is important to use the best estimate of the mean F_y in seismic design, R_yF_y, why not do so in nonseismic design? Also, has the introduction of R_yF_y in AISC 341 met the desired intent when applied?

The AISC task group considered if the increased yield strength modifier, R_y, that is used in AISC 341 should also be included in AISC 360. The actual F_y is, on average, greater than the nominal F_y used in design. This opens the possibility that a compact section based on the nominal F_y may actually be a noncompact section because the λ based on the actual F_y may be less than λ_p based on the nominal F_y. The counterargument is that the design strength based on F_y will be conservatively less than that based on R_yF_y,

Table 6. Comparison of AISC 360 and AISC 341 w/t Limits						
AISC 360 Table B4.1a Compression Elements in Members Subject to Compression Only				AISC 341 Table D1.1		
Case	**Element Description**	λ_r	λ_p	**Note**	λ_{md}	λ_{hd}
1	Rolled I-flanges	$0.56\sqrt{E/F_y}$	—		$0.40\sqrt{E/(R_yF_y)}$	$0.32\sqrt{E/(R_yF_y)}$
2	Built-up I-flanges	$0.64\sqrt{E/F_y}$	—		$0.40\sqrt{E/(R_yF_y)}$	$0.32\sqrt{E/(R_yF_y)}$
3	Angle legs	$0.45\sqrt{E/F_y}$	—		$0.40\sqrt{E/(R_yF_y)}$	$0.32\sqrt{E/(R_yF_y)}$
4	Tee stems	$0.75\sqrt{E/F_y}$	—		$0.40\sqrt{E/(R_yF_y)}$	$0.32\sqrt{E/(R_yF_y)}$
5	I-webs	$1.49\sqrt{E/F_y}$	—	Braces	$1.57\sqrt{E/(R_yF_y)}$	$1.57\sqrt{E/(R_yF_y)}$
6	HSS walls	$1.40\sqrt{E/F_y}$	—	Braces	$0.76\sqrt{E/(R_yF_y)}$	$0.65\sqrt{E/(R_yF_y)}$
			—	Columns	$1.18\sqrt{E/(R_yF_y)}$	$0.65\sqrt{E/(R_yF_y)}$
7	Cover plates	$1.40\sqrt{E/F_y}$	—		—	—
8	Stiffened element	$1.49\sqrt{E/F_y}$	—		—	—
9	Round HSS	$0.11\ E/F_y$	—		$0.062\ E/(R_yF_y)$	$0.053\ E/(R_yF_y)$
	Flanges of H-piles	—	—		$0.48\sqrt{E/(R_yF_y)}$ [a]	n.a.[a]
	Webs of H-piles	—	—		$1.57\sqrt{E/(R_yF_y)}$ [a]	n.a.[a]
AISC 360 Table B4.1b Compression Elements in Members Subject to Flexure						
10	Rolled I-flanges	$1.00\sqrt{E/F_y}$	$0.38\sqrt{E/F_y}$		$0.40\sqrt{E/(R_yF_y)}$	$0.32\sqrt{E/(R_yF_y)}$
11	Built-up I-flanges	$0.95\sqrt{E/F_y}$	$0.38\sqrt{E/F_y}$		$0.40\sqrt{E/(R_yF_y)}$	$0.32\sqrt{E/(R_yF_y)}$
12	Angle legs	$0.91\sqrt{E/F_y}$	$0.54\sqrt{E/F_y}$		$0.40\sqrt{E/(R_yF_y)}$	$0.32\sqrt{E/(R_yF_y)}$
13	Minor axis I-flanges	$1.00\sqrt{E/F_y}$	$0.38\sqrt{E/F_y}$		—	—
14	Tee stems	$1.52\sqrt{E/F_y}$	$0.84\sqrt{E/F_y}$		$0.40\sqrt{E/(R_yF_y)}$	$0.32\sqrt{E/(R_yF_y)}$
15	I-webs	$5.70\sqrt{E/F_y}$	$3.76\sqrt{E/F_y}$		$f(P_u/P_y)$	$f(P_u/P_y)$
16	Singly symmetrical I-webs	$5.70\sqrt{E/F_y}$	$f(h_c/h_p)$		—	—
17	HSS flanges	$1.40\sqrt{E/F_y}$	$1.12\sqrt{E/F_y}$		$1.18\sqrt{E/(R_yF_y)}$	$0.65\sqrt{E/(R_yF_y)}$
18	Flange cover plates	$1.40\sqrt{E/F_y}$	$1.12\sqrt{E/F_y}$		—	—
19	HSS webs	$5.70\sqrt{E/F_y}$	$2.42\sqrt{E/F_y}$		—	—
	Box webs				$1.75\sqrt{E/(R_yF_y)}$	$0.67\sqrt{E/(R_yF_y)}$
20	Round HSS	$0.31E/F_y$	$0.07E/F_y$		$0.062E/(R_y F_y)$	$0.053E/(R_y F_y)$
21	Box flanges	$1.49\sqrt{E/F_y}$	$1.12\sqrt{E/F_y}$		$1.18\sqrt{E/(R_yF_y)}$	$0.65\sqrt{E/(R_yF_y)}$

[a] Potentially better categorized as flexure case in AISC 341.
— Denotes not applicable.

Table 7. Summary of Intended Objectives for Application of λ Limits in AISC 341-16			
	System*	**Element**	**Objective**
λ_{md}	IMF	Beam	M_p, 0.02 rad ID
		Column	R_r
	OCBF	Brace	R_r, n cycles
	MT-SCBF	Strut	M_{pe}
	EBF	Beam outside link	R_r
		Brace	R_r
	BRBF	Beam	R_r
		Column	R_r
λ_{hd}	SMF	Beam	M_p, 0.04 rad ID @ 0.8M_p
		Column	M_p, R_r, 0.04 rad
	STMF	Chord and diagonal	3% ID
		Column	3% ID
	SCCS	Column	M_p, limit FLB, large θ_p
	SCBF	Beam	R_r
		Column	R_r, large θ_p
		Brace	R_r, n cycles, yield @ 0.3%ID, 10–20ε_y
	MT-SCBF	Column	M_{pe}
		Brace	R_r, n cycles, yield @ 0.3%ID, 10–20ε_y
	EBF	Link	0.02–0.08 rad inelastic rotation
		Column	R_r
	MT-BRBF	Beam	R_r
		Column	R_r
	SPSW	Column boundary	R_r
		Horizontal boundary	M_p, n cycles

Note: R_r = required system strength based on capacity design, ID = interstory drift, FLB = flange local buckling.
* See AISC 341 for SFRS abbreviations.

even if the member is no longer compact. This counter argument was found to prevail for all practical cases studied (Schafer et al., 2020). For the structures, loadings, and margin of safety in AISC 360, large overloads are not expected, and the actual mode of failure is not important. This is not true for AISC 341, where structures undergo extreme conditions. In this case, the failure mode could potentially cause the energy-absorbing location to shift from the intended location to an undesirable location, resulting in nonductile failure modes. Therefore, while it is not recommended that R_y be included in AISC 360, it is appropriate to include R_y in AISC 341.

Use of R_yF_y in the w/t limits for AISC 341 provides a more accurate prediction of the desired behavior; further, it removes the perverse incentive of specifying a lower F_y, even when expected F_y is high, only so that a compactness limit or other limit related to energy dissipation can be met. However, the implementation of the R_y factor in the existing w/t limits requires discussion. AISC 341 introduced R_y into its w/t limits in the 2016 edition for the first time, but in such a manner as to not actually change the limiting values for typical steels. For example, $\lambda_{md} = 0.38\sqrt{E/F_y}$ for flanges of I-shaped sections in AISC 341-10 was converted to $0.40\sqrt{E/(R_yF_y)}$ in AISC 341-16 by assuming R_y = 1.1 for A992-type steel. Similarly, for walls of rectangular HSS used as diagonal braces $\lambda_{hd} = 0.55\sqrt{E/F_y}$ for flanges of I-shaped sections in AISC 341-10 was converted to $0.65\sqrt{E/(R_yF_y)}$ in AISC 341-16 by assuming R_y = 1.14 for A500 Grade B steel.

For the former example, the original experimental source for the λ_p limit (Lukey and Adams, 1969), which

λ_{md} is based on, was experimentally developed based on measured F_y but then applied in AISC 360, and later in AISC 341, as nominal/specified F_y. In general, researchers develop w/t limits with measured F_y properties and code committees then implement them with specified properties. If the change in 2016 for AISC 341 was intended to bring the w/t limit in line with the original testing, then the coefficient should not have been modified and only R_y added to the denominator. The task group recommended that course of action and it is expected in the forthcoming 2022 edition of AISC 360. Schafer et al. (2020) provides additional discussion on R_y and the impact of other material properties (strain hardening slope, etc.) and higher strength steels on the w/t limits.

Web-Flange Interaction and Impact on Seismic *w/t* Limits (Deep Columns)

Deep wide-flange columns have seen increasing use in the SFRSs of buildings, particularly in moment frames due to their relative effectiveness for story drift control. Columns in an SMF are expected to experience flexural yielding and form a plastic hinge at the column base. Deep columns have h/t_w ratios that often are significantly higher than those of shallow columns (e.g., W12 or W14). Recent testing of λ_{hd}-compliant deep columns at the University of California–San Diego (UCSD) has shown that the web in these columns was not effective in stabilizing the flanges under cyclic loading (Ozkula and Uang, 2015; Chansuk et al., 2018). Interactive web-flange local buckling occurs prematurely and causes significant strength degradation and axial shortening. Under cyclic loading, lateral-torsional buckling, together with local buckling, can also occur. Figure 4 illustrates two typical stability driven failures observed in the testing. Independent research conducted by Elkady and Lignos (2018) and Wu et al. (2018) have also confirmed this problematic phenomenon in deep columns for moment frames.

To resolve this issue, new λ_{hd} and λ_{md} limits have been proposed for AISC 341 to be used in beams, columns, or links as webs in flexure, or as combined axial and flexure, including webs of rolled or built-up I-shaped sections or channels, side plates of boxed I-shaped sections, and webs of built-up box sections as provided in Table 8. The new limits are based on regression analysis of deep column responses from both testing and finite element simulation and consider the effects of boundary condition and lateral loading sequence on local and lateral-torsional buckling (Ozkula et al., 2021). The limiting h/t_w ratios are developed for constant axial loads. For exterior columns with varying axial loads due to the overturning moment effect, the proposed limits are conservative.

ALTERNATIVES TO LOCAL BUCKLING (*w/t*) LIMITS

The task group was also charged with commenting on alternative means of establishing basic local buckling performance objectives and ensuring the specification provides user pathways to these alternative means when current w/t limits may be an impediment—for example, for higher strength steels, steels with nontraditional stress-strain relations (e.g., no yield plateau like stainless steel), unusual built-up cross sections, etc.

Cross-Section Local Slenderness Limits and Application of DSM

The direct strength method (DSM) (Schafer, 2019) as implemented in AISI S100 provides limits that are similar in spirit to the AISC w/t limits, but for the entire cross section, where $P_{cr\ell}$ is the elastic axial local buckling force and $M_{cr\ell}$ is the elastic flexural local buckling moment. Cross-section elastic local buckling may be determined by analytical formulas for common shapes (e.g., Gardner et al., 2019; Seif and Schafer, 2010) or numerical analyses for more complex configurations as detailed in the AISI S100 Commentary.

$$P_n = P_y \quad \text{if} \quad \lambda_\ell^* = \sqrt{\frac{P_y}{P_{cr\ell}}} = 0.776 \tag{11}$$

(a) W24×131 column

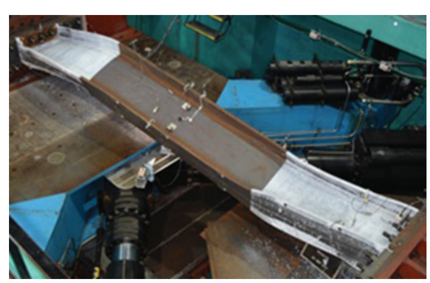

(b) W24×176 column

Fig. 4. Typical deep column buckling mode.

Table 8. Proposed Change in Web w/t in AISC 341		
	λ_{hd} for Highly Ductile Members	λ_{md} for Moderately Ductile Members
AISC 341-16	For $C_a \le 0.114$: $2.57\sqrt{\frac{E}{R_yF_y}}(1-1.04C_a)$ For $C_a > 0.114$: $0.88\sqrt{\frac{E}{R_yF_y}}(2.68-C_a) \ge 1.57\sqrt{\frac{E}{R_yF_y}}$	For $C_a \le 0.114$: $3.96\sqrt{\frac{E}{R_yF_y}}(1-3.04C_a)$ For $C_a > 0.114$: $1.29\sqrt{\frac{E}{R_yF_y}}(2.12-C_a) \ge 1.57\sqrt{\frac{E}{R_yF_y}}$
Proposed for AISC 341-22	$2.5(1-C_a)^{2.3}\sqrt{\frac{E}{R_yF_y}}$	$5.4(1-C_a)^{2.3}\sqrt{\frac{E}{R_yF_y}}$
Note: $C_a = \frac{\alpha_s P_r}{R_y F_y A_g}$ and P_r is the required axial strength, α_s is the ASD/LRFD conversion factor, and A_g is the gross area of the column; all other terms previously defined.		

$$M_n = M_y \quad \text{if} \quad \lambda_\ell^* = \sqrt{\frac{M_y}{M_{cr\ell}}} = 0.776 \tag{12}$$

$$M_n \cong M_p \quad \text{if} \quad \lambda_\ell^* = \sqrt{\frac{M_y}{M_{cr\ell}}} = 0.086 \tag{13}$$

Equations 11 and 12 provide the equivalent to the λ_r limit and Equation 13 the λ_p limit. Equation 13 is intentionally conservative in its application for AISI S100 and would need modification for AISC 360 application.

Cross-Section Local Slenderness Limits and Application of CSM

The continuous strength method (CSM) developed by Gardner et al. (e.g., Afshan and Gardner, 2013; Zhao et al., 2017) provides a complete strain-based alternative to local buckling classification limits, but it could equally be used to provide basic limits. The CSM base curve implies the maximum strain capacity is a function of the local buckling slenderness, focusing on the range where $\varepsilon \ge \varepsilon_y$:

$$\varepsilon = \frac{0.25}{\lambda_\ell^{*3.6}}, \quad \lambda_\ell^* = \sqrt{\frac{P_y}{P_{cr\ell}}} \text{ or } \sqrt{\frac{M_y}{M_{cr\ell}}} \tag{14}$$

If we set $\varepsilon = \varepsilon_y$ for the equivalent to the λ_r limit, and set $\varepsilon = 4\varepsilon_y$ for the λ_p limit:

$$P_n = P_y \quad \text{if} \quad \lambda_\ell^* = \sqrt{\frac{P_y}{P_{cr\ell}}} = 0.68 \tag{15}$$

$$M_n = M_y \quad \text{if} \quad \lambda_\ell^* = \sqrt{\frac{M_y}{M_{cr\ell}}} = 0.68 \tag{16}$$

$$M_n \cong M_p \quad \text{if} \quad \lambda_\ell^* = \sqrt{\frac{M_y}{M_{cr\ell}}} = 0.46 \tag{17}$$

Note $\varepsilon = 15\varepsilon_y$ for the λ_{hd} limit would result in $\lambda_\ell^* = 0.32$. Given the approximate nature of current element slenderness limits, it should be permitted to use more robust cross-section-based slenderness limits when desired by the engineer. Note that for some sections under some loading conditions, these limits will be more stringent than current practice and for others more lenient. In general, the large class of w/t limits (Table B4.1 in AISC 360 and Table D1.1 in AISC 341) could be replaced with these simple cross-section-based criteria.

An additional note on Equation 14: The power of this expression should not be understated. Recall Equation 6 where the elastic plate buckling strain was made independent of Young's modulus; so too is Equation 14 and, in fact, has been developed considering stainless steel, aluminum, and traditional mild carbon steels. Further, the limits in Equations 15–17 agree quite well with Winter's (1947) insights and Haiijer and Thurlimann's (1960) insights on key slenderness ranges for first yield and plastic behavior. This generalization is attractive, and a means to leverage this insight is worthy of consideration for AISC *Specifications*.

Extensions on the Use of CSM and DSM

Both CSM and DSM can do more than provide the local buckling limits; they can be used to predict the actual cross-section strength. CSM's strain-based approach is particularly powerful if nonlinearity in the material stress-strain curve is such that the elastic-plastic assumption is not adequate (as is the case with some new high-strength steel grades). Both CSM and DSM have been developed and are being adopted for forthcoming editions of stainless steel standards (ASCE, 2021; AISC, 2021).

In addition, Torabian and Schafer (2014) used a CSM-inspired approach to establish rotation capacity in addition to strength. Thus, it is possible to provide a methodology for predicting allowable rotation capacity, R_{cap}, for use in material nonlinear analyses, both static for AISC 360 and potentially dynamic for application to AISC 341. This could potentially be advanced in AISC 360, Appendix 1. Recent work of Gardner et al. (2019) has extended these insights directly into line elements for use in system analysis.

DISCUSSION AND RECOMMENDATIONS

The current w/t formulation—for example, Equation 4—for local bucking limits in AISC 360 and AISC 341 has several strengths: The method (1) is easy and fast to apply, (2) has a long tradition of use, (3) has a relatively high level of clarity, and (4) leads to reliable strength predictions. Weaknesses of the existing w/t formulation include the following: (1) The method connects to the element, not the section, and most behavior objectives are at the section level; (2) for the limits to be simple, constant coefficients for C (Equation 4) are commonly used; however, if web-flange interaction (i.e., simple equilibrium and compatibility within the section), stress distribution (e.g., stresses from a beam-column, difference in stresses when a flange tip is in tension/compression), or material nonlinearity is considered, this breaks down, and determination of C becomes its own quite complex process; and (3) by using w/t instead of the nondimensional slenderness, λ^* (i.e., $\sqrt{F_y/F_{cr}}$), the limits appear to be different for every element (i.e., lots of different C values), while in reality, only one assumption (λ^*) is typically being made—this reduces conceptual clarity. In addition, when one delves into the details, such as Table 3 and Table 4, numerous small inconsistencies emerge. Comparing the level of detail required to understand current provisions with the alternative local buckling criteria discussed earlier, it is evident that clearer, more robust, and more direct methods are now available based on cross-section local buckling instead of element local buckling to achieve the same objectives as current methods.

The task group came to the following recommendations:

Nonseismic AISC 360 Recommendations

Rewrite the AISC 360, Table B4.1 Commentary. Provide objectives using the *Objective of AISC 360 Local Buckling Limits* section of this paper (aligned with the *Specification*, not aspirational). Make the role of nondimensional slenderness, λ^*, clear, and provide finalized versions of Tables 3 and 4 in the AISC 360 Commentary or through reference to an archival publication.

Provide an alternative pathway for the use of cross-section elastic buckling analysis that includes web-flange interaction as an alternative to current w/t limits. Set $\lambda_r^* = 0.7$ or 1.0 as appropriate and $\lambda_p^* = 0.5$ for these alternative provisions. Current λ_r for flexure limits should be recast to make it explicitly clear why $\lambda_r^* = 1.0$ not $\lambda_r^* = 0.7$ is used. This would explain the discrepancy in Table B4.1b between (1) stiffened elements in compression and (2) unstiffened elements in compression and stiffened elements in flexure and explain the discrepancy between compression elements in Table B4.1a and b. This would also explain a significant discrepancy between current AISC practice and other international standards. Assuming independent research is not conducted, then it is recommended that $\lambda_r^* = 0.7$ be used throughout and AISC 360, Chapter F, modified to accommodate this change. This would remove the discrepancy in Table B4.1b between (1) stiffened elements in compression and (2) unstiffened elements in compression and stiffened elements in flexure and would remove the discrepancy between compression elements in Table B4.1a and b. This would also remove a significant discrepancy between current AISC practice and other international standards.

With respect to the compact limit λ_p, it is recommended that this limit be split into λ_{p1} and λ_{p2} consistent with Eurocode Class 1 and Class 2 that provide M_p with minimum rotation and M_p, respectively. This will provide improved efficiency in some cases and will provide needed rotation capacity only where necessary—for example, in inelastic analysis with moment redistribution of AISC 360, Appendix 1. It is recommended that for simplicity, implementation in Chapter F need only use λ_{p2} since this establishes M_p, while AISC 360, Appendix 1, could reference the use of λ_{p1} for plastic design and/or material nonlinear analyses with redistribution.

In addition, the following is recommended: Align λ_p Case 12 (angle) with that of Case 10 (rolled flange in compression) or make it explicit that Case 12 only applies to the angle leg under stress gradient. Align λ_p Case 15 (I-section web) with that of Case 19 (box-section web) or provide evidence that I-section webs can have more liberal w/t limits than box-section webs (even beyond that of assuming a fully fixed edge boundary condition for the I-section web). Remove the use of residual stress (F_L vs. F_y) in the Table B4.1 limits. As needed, correct application of limits in Chapter F after removal to ensure new limits are not unduly conservative.

Seismic AISC 341 Recommendations

The task group recommendations for AISC 341 include rewriting the Table D1.1 Commentary: Provide objectives from the *Objectives* section of this paper (aligned with the *Specification*, not aspirational) and the finalized version of Table 7 in the Commentary or reference to archival publication. Note: The Commentary should describe intent and not imply specific values that are met by the w/t limits. Correct the λ_{md} and λ_{hd} limits back to their 2010 coefficients (and include R_y). Provide an alternate pathway for the use of cross-section elastic buckling analysis that includes web-flange interaction as an alternative to current *w*/*t* limits. Set $\lambda^*_{md} = 0.5$ and $\lambda^*_{hd} = 0.32$ for these alternative provisions. Adopt the proposed provisions for deep columns provided earlier.

Additional Recommendations

A number of additional recommendations are also provided. Establish a research project to take advantage of the findings from the continuous strength method research and bring these advantages into the AISC 360 and AISC 341 standards. Active work in the development of AISC 370, *Specification for Structural Stainless Steel Buildings* (2021), may be utilized in this regard. Establish a research project to determine cyclic degradation in the strain capacity of plate elements subjected to local buckling such that AISC 341 *w*/*t* criteria can be improved. Recent advances in cyclic fracture models of ductile steels can be leveraged as a mechanical basis for this effort, and the results have the potential to widely influence λ_{md} and λ_{hd} and their future application. Develop a test standard for establishing *w*/*t* limits (for AISC 360 and AISC 341) consistent with past practice and current application. This recommendation provides a pathway for alternative built-up shapes and new materials (steels) that may be impeded by current design rules. Extend AISC 360, Appendix 1, to provide alternative means for meeting λ_{pd} criteria based on cross-section slenderness, provide discussion/guidance on member rotational demands coming from nonlinear analysis, and show how to calculate member rotational capacity based on local cross-section slenderness.

CONCLUSIONS

Cross-section width-to-thickness limits are a longstanding and reliable means to ensure behavioral objectives related to the local buckling performance of structural steel members. Establishing the underlying assumptions inherent in current width-to-thickness limits developed over the course of the last 80+ years is critical to advancing structural steel design for new steels and configurations. Existing width-to-thickness limits are presented in AISC *Specifications* in a manner suggesting each limit is unique to each element and loading, while actual limits are based on a small number of targeted, nondimensional plate slenderness regimes, where the nondimensional plate slenderness, λ^*, is defined based on the square root of the yield stress divided by the critical elastic plate buckling stress. Alternative methods that employ λ^* for local buckling of the complete cross section are capable of providing local buckling limits similar to current practice, but with greater simplicity and generality, and are worth considering as alternative means of meeting local buckling-based behavioral objectives for both nonseismic and seismic local buckling limits. Seismic width-to-thickness limits provide for objectives far beyond strength and are used extensively to ensure ductility and avoid premature fracture in a variety of different seismic force-resisting systems. Proposals to improve current seismic width-to-thickness limits to account for the expected yield stress of the material and to handle web-flange interaction in local buckling of columns in moment frames are specifically addressed and recommendations provided. A series of recommendations spanning from practical—for example, provide two levels of compact section criteria to parallel Eurocode's Class 1 and Class 2 sections and adopt proposed provisions for deep columns in moment frames—to longer term—for example, provide alternative pathways for establishing local buckling limits are provided. This review of the current status of local buckling width-to-thickness limits was conducted by an ad hoc task group of the AISC Committee on Specifications during the development cycle for the 2022 editions of AISC 360 and AISC 341.

ACKNOWLEDGMENTS

This paper is based on the work conducted by the AISC Task Group: Local Buckling (Width-to-Thickness Limits), which operated from 2017 to 2019 under the AISC Committee on Specifications (COS) with Ben Schafer as chair; Tim Fraser, Subhash Goel, Pat McManus, Don Sherman, Tom Sabol, Chia-Ming Uang, and Amit Varma as members; and Brent Leu as secretary. Additional AISC COS members and guests contributed at the in-person meetings as guests of the Task Group. In particular, Lou Geschwindner, Perry Green, Kerry Kreitman, and Don White all contributed substantially to the Task Group's work. All contributions and efforts of the Task Group members and friends are acknowledged and thanked by the authors.

REFERENCES

AASHTO (2017), *LRFD Bridge Design Specification*, 8th Ed., American Association of State Highway and Transportation Officials, Washington, D.C.

Afshan, S. and Gardner, L. (2013), "The Continuous Strength Method for Structural Stainless Steel Design," *Thin-Walled Structures*, Vol. 68, pp. 42–49. doi:10.1016/j.tws.2013.02.011.

AIJ (2010), *Recommendation for Limit State Design of Steel Structures*, Architectural Institute of Japan.

AISC (1986), *Load and Resistance Factor Design Specification for Structural Steel Buildings*, American Institute of Steel Construction, Chicago, Ill.

AISC (1990), *Seismic Provisions for Structural Steel Buildings*, American Institute of Steel Construction, Chicago, Ill.

AISC (1999), *Load and Resistance Factor Design Specification for Structural Steel Buildings*, American Institute of Steel Construction, Chicago, Ill.

AISC (2010), *Seismic Provisions for Structural Steel Buildings*, ANSI/AISC 341-10, American Institute of Steel Construction, Chicago, Ill.

AISC (2016a), *Seismic Provisions for Structural Steel Buildings*, ANSI/AISC 341-16, American Institute of Steel Construction, Chicago, Ill.

AISC (2016b), *Specification for Structural Steel Buildings*, ANSI/AISC 360-16, American Institute of Steel Construction, Chicago, Ill.

AISC (2021), *Specification for Structural Stainless Steel Buildings*, ANSI/AISC 370-21, American Institute of Steel Construction, Chicago, Ill.

AISI (2016), *North American Specification for the Design of Cold-Formed Steel Structural Members*, AISI S100-16, American Iron and Steel Institute, Washington, D.C.

Allen, H.G. and Bulson, P.S. (1980), *Background to Buckling*, McGraw-Hill, New York, N.Y.

ASCE (2021), *Specification for the Design of Cold-Formed Stainless Steel Structural Members*, SEI/ASCE 8-21, American Society of Civil Engineers, Reston, Va.

CEN (2004), *Eurocode 3: Design of Steel Structures*, EN 1993-1-1 2004, Comite Européen de Normalisation, Brussels, Belgium.

Chansuk, P., Ozkula, G., and Uang, C.-M. (2018), "Seismic Behavior and Design of Deep, Slender Wide-Flange Structural Steel Beam-Column Members: Phase 2," Report No. SSRP-18/02, Department of Structural Engineering, University of California, San Diego, La Jolla, Calif.

Elkady, A. and Lignos, D.G. (2018), "Full-Scale Testing of Deep Wide-Flange Steel Columns under Multi-Axis Cyclic Loading: Loading Sequence, Boundary Effects and Out-of-Plane Brace Force Demands," *Journal of Structural Engineering*, Vol. 144, No. 2.

Fieber, A., Gardner, L., and Macorini, L. (2019), "Design of Structural Steel Members by Advanced Inelastic Analysis with Strain Limits," *Engineering Structures*, Vol. 199. doi:10.1016/j.engstruct.2019.109624.

Gardner, L., Fieber, A., and Macorini, L. (2019), "Formulae for Calculating Elastic Local Buckling Stresses of Full Structural Cross-Sections," *Structures*, Vol. 17, pp. 2–20. doi:10.1016/j.istruc.2019.01.012.

Haaijer, G. and Thurlimann, B., (1960), "On Inelastic Buckling in Steel," *Proceedings ASCE*, 84 (EM2), p. 1581 [also *Transactions ASCE*, Vol. 125 (1960), Reprint No. 124 (60-2), (1960)], Fritz Laboratory Reports, Paper 1,426.

ICBO (1988), *Uniform Building Code*, International Council of Building Officials, Whittier, Calif.

Johnson, D. (1976), "Buckling of Beam Compression Flanges," Report to American Iron and Steel Institute.

Lukey, A.F., and Adams, P.F. (1969), "The Rotation Capacity of Beams under Moment Gradient," *Journal of the Structural Division*, ASCE, Vol. 95, No. 6, pp. 1,173–1,188.

Ozkula, G. and Uang, C.-M., (2015), "Seismic Behavior and Design of Deep, Slender Wide-Flange Structural Steel Beam-Column Members: Phase 1," Report No. SSRP-15/06, Department of Structural Engineering, University of California, San Diego, La Jolla, Calif.

Ozkula, G., Uang, C.-M., and Harris, J. (2021), "Development of Enhanced Seismic Compactness Requirement for Webs in Wide-Flange Steel Columns," *Journal of Structural Engineering* (accepted).

Salmon, C., Johnson, J., and Malhas, F. (2009), *Steel Structures: Design and Behavior*, 5th Ed., Pearson, New York.

Schafer, B.W. (2019), "Advances in the Direct Strength Method of Cold-Formed Steel Design," *Thin-Walled Structures*, Vol. 140, pp. 533–541. doi:10.1016/j.tws.2019.03.001.

Schafer, B.W., Fraser, T. Goel, S., McManus, P., Sherman, D., Sabol, T., Uang, C.-M., and Varma, A. (2020), "Task Group Report on Local Buckling (Width-to-Thickness) Limits," prepared by the AISC Committee on Specifications Ad Hoc Task Group on Local Buckling (Width-to-Thickness) Limits, January 7, AISC, Chicago, Ill.

Seif, M. and Schafer, B.W. (2010), "Local Buckling of Structural Steel Shapes," *Journal of Constructional Steel Research*, Vol. 66, pp. 1,232–1,247.

Torabian, S. and Schafer, B.W. (2014), "Role of Local Slenderness in the Rotation Capacity of Structural Steel Members," *Journal of Constructional Steel Research*, Vol. 95, pp. 32–43.

White, D.W. (2008), "Unified Flexural Resistance Equations for Stability Design of Steel I-Section Members: Overview," *Journal of Structural Engineering*, ASCE, Vol. 134, No. 9, pp. 1,405–1,424.

Wilkinson, T. and Hancock, G.J. (1998), "Tests to Examine Compact Web Slenderness of Cold-Formed RHS," *Journal of Structural Engineering*, ASCE, Vol. 124, No. 10, pp. 1,166–1,174.

Winter, G. (1947), "Strength of Thin Steel Compression Flanges," *Transactions of the American Society of Civil Engineers*, Vol. 112, No. 1, pp. 527–554.

Wu, T.Y., El-Tawil, S., and McCormick, J. (2018), "Highly Ductile Limits for Deep Steel Columns," *Journal of Structural Engineering*, ASCE, Vol. 144, No. 4, 04018016.

Zhao, O., Afshan, S., and Gardner, L. (2017), “Structural Response and Continuous Strength Method Design of Slender Stainless Steel Cross-Sections,” *Engineering Structures*, Vol. 140, pp. 14–25. doi:10.1016/j.engstruct.2017.02.044.

Ziemian, R. (2010), *Guide to Stability Design Criteria for Metal Structures*, 6th Ed., Wiley, New York, N.Y.